

# Direct experimental visualization of atomic and electron dynamics with attosecond pulses

C D Lin<sup>1</sup>, X M Tong<sup>2,3</sup> and Toru Morishita<sup>4</sup>

<sup>1</sup> J R Macdonald Laboratory, Physics Department, Kansas State University, Manhattan, KS 66506-2604, USA

<sup>2</sup> Institute of Materials Science, Graduate School of Pure and Applied Science, University of Tsukuba, 1-1-1 Tennodai, Tsukuba, Ibaraki 305-8573, Japan

<sup>3</sup> Center for Computational Sciences, University of Tsukuba, 1-1-1 Tennodai, Tsukuba, Ibaraki 305-8577, Japan

<sup>4</sup> Department of Applied Physics and Chemistry, University of Electro-Communications, Chofu-shi, Tokyo 182-8585, Japan

Received 22 December 2005, in final form 26 December 2005

Published 22 June 2006

Online at [stacks.iop.org/JPhysB/39/S419](http://stacks.iop.org/JPhysB/39/S419)

## Abstract

We illustrate how attosecond light pulses can be used directly in mapping out the time dependence of the motion of atoms in a small molecule, as well as of the correlated motion of two excited electrons in an atom. For simple molecules such as H<sub>2</sub> and D<sub>2</sub>, we show that the vibrational wave packet can be mapped out very accurately, including details due to the broadening and interference. For doubly excited states of a helium atom, we show that the time-dependent correlated motion between the two electrons can be mapped via double ionization with attosecond pulses.

(Some figures in this article are in colour only in the electronic version)

## 1. Introduction

One of the central problems in modern physics and chemistry is the development of methods for controlling the outcome of a physical or chemical process. In the domain of ultrashort laser pulses, with pulse durations of tens to hundreds of femtoseconds, it has been demonstrated in the last decade that the coherent properties of the lasers can be used to manipulate the motion of electrons and nuclei, thus creating favourable pathways where specific chemical reactions can be enhanced [1]. With the recent developments of ultrashort XUV (extreme ultraviolet) light pulses with durations of several hundred attoseconds, naturally it is interesting to ask what new insights of the microscopic world can be gained with these new tools that are becoming available. Since the typical time scale of the electronic motion in the ground and the lower excited states of atoms and molecules are in the order of hundreds of attoseconds, it is expected that attosecond XUV pulses be used to probe as well as to control the motion of electrons in an atom or molecule.

To manipulate the reaction pathways at increasing shorter time scale, knowledge of the time evolution of the complete wave packet is essential. In this paper we illustrate two examples of the possible use of attosecond pulses for determining the time evolution of the wave packets. The first example deals with the wave packets of  $\text{H}_2^+$  and  $\text{D}_2^+$  molecules. For these simple molecules, their vibrational periods are about 15 fs and 22 fs, respectively. In this case attosecond pulses are used by taking advantage of their broad energy spectrum such that the whole wave packet can be probed from different parts of the internuclear distances at the same time. In the second example, attosecond pulses are used to probe the dynamics of the correlated motion of two excited electrons. In this case, attosecond pulses are indispensable since the time scale involving electronic interactions is in the order of tens to hundreds of attoseconds.

## 2. Complete mapping of the vibrational wave packet of $\text{D}_2^+$ ions using attosecond XUV pulses

To determine the time-dependent wave packets, various pump–probe techniques have been suggested. For dissociating molecules, a direct method is to map out the time-dependent kinetic energy release (KER) of the ions following Coulomb explosion after the probe pulse. For the wave packets of  $\text{H}_2^+$  and  $\text{D}_2^+$  molecules, laser pulses of durations of about 80 fs [2], 50 fs [3], and more recently, of 25 fs [4], have been used in pump–probe experiments. As noted earlier, since the vibrational periods of these two molecules are about 15 fs and 22 fs, respectively, many interesting features of the time-dependent wave packets disappear when they are probed with these long pulses. Glimpse of the wave packet evolution does appear in the recent experiment of Alnaser *et al* [5] where they used two 8 fs pulses to double ionize  $\text{H}_2$  or  $\text{D}_2$ . By measuring the KER of the fragmented ions versus time delay, ‘movies’ showing the motion of the wave packets on the two lowest potential surfaces have been constructed. However, details of the wave packet motion still cannot be extracted from these experiments. In particular, the vibrational distributions of the initial wave packet remain unexplored. Using attosecond XUV pulses, with its ‘white’ light and its short duration, we will show that detailed information of the vibrational wave packet can be determined directly from experiments. Such experiments would offer the opportunity to study how the creation of the initial wave packet depends on the shaped pulses, for example, thus gaining full coherent control in future pump–probe experiments.

The basic idea for such an experiment is this: a short pump pulse is used to create a wave packet by ionizing the  $\text{D}_2$  molecule. For simplicity, we assume that  $\text{D}_2^+$  is created only in the ground  $1\sigma_g$  electronic state, together with an initial vibrational wave packet. This wave packet will propagate in the  $1\sigma_g$  potential curve of  $\text{D}_2^+$ . We model that the wave packet was created at  $\tau = 0$  following the Franck–Condon principle. With this initial wave packet which is the ground vibrational wavefunction of the  $\text{D}_2$  molecule, the time evolution of this wave packet can be trivially calculated. The top frame of figure 1 shows the density plots of its time evolution.

The middle frame shows the result of the simulated wave packet reconstructed from the KER when the wave packet is probed with a 300 attosecond pulse with mean energy of 50 eV. The bottom frame shows the reconstructed wave packet if it is probed with an 8 fs IR laser pulse, with mean wavelength of 800 nm at an intensity of  $9 \times 10^{14} \text{ W cm}^{-2}$ . The latter result is consistent with the observation of Alnaser *et al* [5].

To obtain theoretical KER spectra by attosecond pulses, we assume that the intensity is of the order of  $10^{12} \text{ W cm}^{-2}$ . In this case ionization can be calculated using first-order

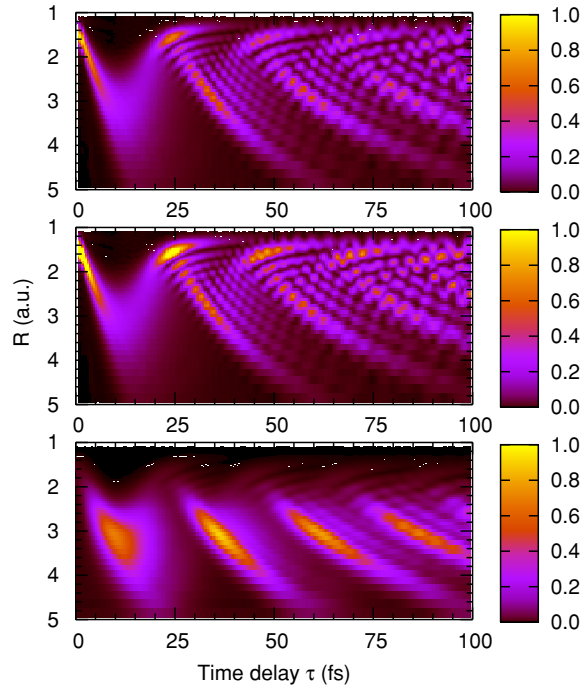


**Figure 1.** Time evolution of the density distribution of the  $D_2^+$  vibrational wave packet after ionizing  $D_2$  at  $\tau = 0$ , assuming Franck–Condon principle. (a) ‘Exact’ theoretical wave packet (top frame); (b) reconstructed wave packet from probing with a 0.3 fs XUV pulse with centre energy at 50 eV (middle frame); and (c) reconstructed wave packet from probing with an 8 fs, 800 nm IR laser with intensity  $9 \times 10^{14} \text{ W cm}^{-2}$  (bottom frame). The middle frame shows that wave packets are reconstructed in verbatim when probed with attosecond XUV pulses.

perturbation theory. The ionization probability is given by

$$P_{\text{ion}}(R) \propto \int_{E_b}^{\infty} \sigma(E_b, \omega) I(\omega) d\omega, \quad (1)$$

with  $E_b$  the ionization potential of  $D_2^+$  at a given  $R$ , and  $\sigma(E_b, \omega)$  the photoionization cross section by a monochromatic photon of frequency  $\omega$ . The laser pulse is assumed to be Gaussian. Since photoionization cross sections  $\sigma(E_b, \omega)$  at a fixed  $R$  are not conveniently available we used the scaled hydrogen-like photoionization cross sections of atoms [6]

$$\sigma(E_b, \omega) = \frac{2^7}{3Z_s^2} \frac{1}{(1 + \alpha^2)^4} \times \frac{e^{-4/\alpha \tan^{-1}\alpha}}{1 - e^{-2\pi/\alpha}} \quad (2)$$

where  $\alpha = \sqrt{\omega/E_b - 1}$  and  $Z_s = \sqrt{2E_b}$ .

Since the ionization potential is relatively constant except in the small- $R$  region, the photoionization cross sections do not vary much within the range of  $R$  of interest. To obtain the ionization rate from a wave packet at time  $\tau$  after the pump pulse, we calculated

$$\frac{dP(R, \tau)}{dR} \propto |\chi_g(R, \tau)|^2 P_{\text{ion}}(R) \quad (3)$$

where  $\chi_g(R, \tau)$  is the vibrational wave packet at time  $\tau$ . The experimentally measured KER spectra per unit energy are obtained from

$$\frac{dP(E, \tau)}{dE} = R^2 \frac{dP(R, \tau)}{dR}. \quad (4)$$

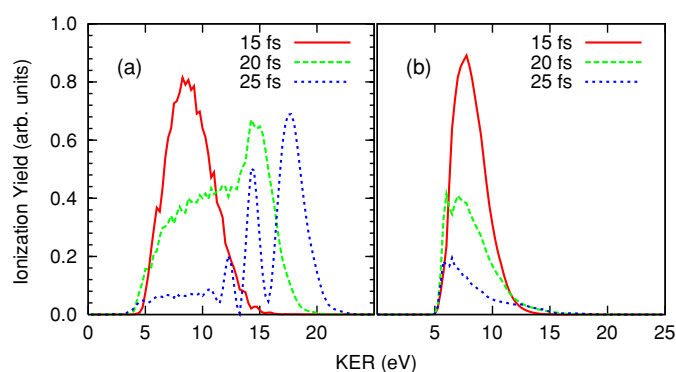


**Figure 2.** Simulated ‘experimental’ total KER spectra of the two  $D^+$  ions at three time delays, from probing the wave packet of  $D_2^+$  by ionizing with (a) a 300 attosecond XUV pulse and (b) an 8 fs IR laser with intensity at  $9 \times 10^{14} \text{ W cm}^{-2}$ .

In this calculation the  $D_2^+$  ion is assumed to be stationary during the probe. This is certainly valid for a 0.3 fs pulse.

For comparison if the probe pulse is an 8 fs IR laser with intensity of  $10^{14}$  to  $10^{15} \text{ W cm}^{-2}$ , then

$$\frac{dP(R, \tau)}{dR} \propto \int W[R, E(t)] |\chi_g(R, t + \tau)|^2 dt. \quad (5)$$

Here  $W$  is the static tunnelling ionization rate of  $D_2^+$  when the internuclear distance is  $R$  and the field strength of the probe laser is  $E(t)$ . For such a ‘long’ pulse, the ionization rate has to be integrated over the pulse duration. The static tunnelling ionization rate  $W$  has been calculated using the complex rotation method [7].

In figures 2(a) and (b) we show the typical KER spectra calculated when the probe pulse is an attosecond pulse or an 8 fs laser, respectively. This is the expected KER spectra, to be obtained from experiments, if the initial wave packet was created following the F–C principle. The spectra were taken at  $\tau = 15, 20$  and  $25$  fs after the pump pulse is over. Clearly with attosecond pulses, the KER spectra show many fine structures, and the energy profile shifts with the time delay. In contrast, the KER spectra from the 8 fs laser probe are limited to a fixed energy range of 5–12 eV. By changing the time delay, only the yield is changed. For such laser pulses, ionization is through tunnelling which decreases exponentially with increasing ionization potentials. This results in, as shown in the bottom frame of figure 1, that the wave packet is probed only when the internuclear distance is around 3–4 au. In contrast, with an attosecond XUV pulse, the whole range of the wave packet is mapped out, as shown in the middle frame of figure 1.

To illustrate that the time evolution of the full wave packet indeed contains many detailed information on the initial state, in figure 3 we show the theoretical  $H_2^+$  wave packet evolution with two different initial conditions. First, the initial vibrational distribution is the same as was given by the Franck–Condon principle. Second, the initial vibrational distributions are given as in the measurement of Urbain *et al* [8]. Clearly the time evolutions of the two wave packets are significantly different, and these differences can be probed with an attosecond pulse.

The ability to readily mapping out the whole wave packet in the time domain also points out that the many roles attosecond pulses will play in chemistry. One can study directly how the initial wave packet depends on the light field of the pump laser, thus paving the way for creating designer’s wave packets to follow favourable reaction paths. For example, can one

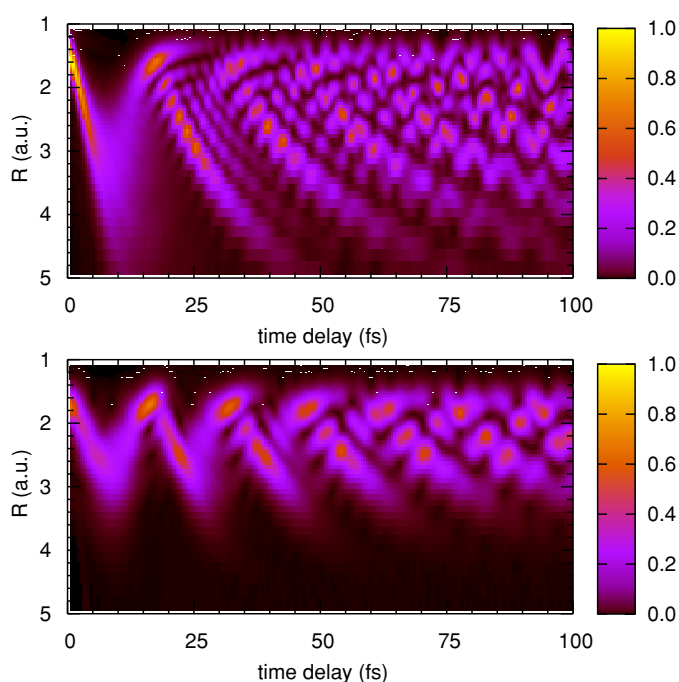


**Figure 3.** Time evolution of the density distribution of the  $\text{H}_2^+$  vibrational wave packet after ionizing  $\text{H}_2$  at  $\tau = 0$ , (a) assuming Franck–Condon distribution (top frame) and (b) by using the vibrational distribution from experiment [8] (bottom frame).

create a wave packet so that it does not spread so quickly as in the present simulation, i.e., closer to a coherent state in a harmonic oscillator? With simple feedback algorithms, it may be possible to do so experimentally in real time. Since the attosecond pulses can map out the wave packet so faithfully, other time dependence studies should be possible, including the interaction of the wave packet with its environment, and its loss of coherence with time, especially in a condensed medium.

### 3. Probing the rovibrational motion of two correlated electrons

The time scale of electronic motion in the ground and the lower excited states of an atom or molecule is in the range of tens to hundreds of attoseconds. Thus it is natural that attosecond pulses be used to probe the time dependence of electron dynamics. Unlike molecules where the time-dependent rotational and vibrational motions have clear classical meaning, the significance of the time dependence of the electronic motion is elusive. The root of this misapprehension lies in the shell model of atoms. According to this model, each electron is moving in an effective central-field potential made of the electron–nucleus interaction plus an average potential due to the remaining electrons. Thus the time dependence of the interaction of one electron with the others is often probed in the form of a relaxation, which tends to be monotonic. Standard atomic structure theory accounts for the deviations of the central field model in terms of configuration interaction (CI). Thus in the time-domain study of electron dynamics, the time-dependent CI coefficients are calculated. Unfortunately such coefficients carry little physical meaning.

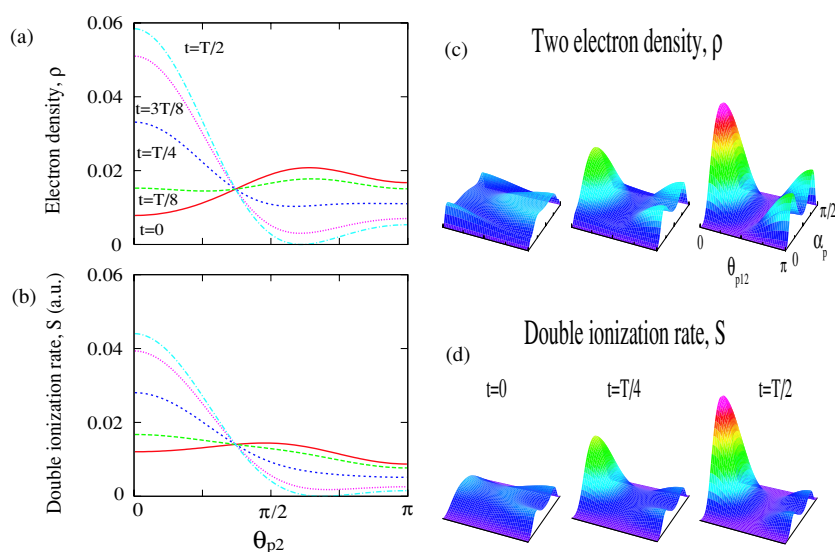


**Figure 4.** Time dependence of double ionization from a coherent state of  $[\varphi(2s^2\ ^1S^e) + \varphi(2p^2\ ^1S^e)]/\sqrt{2}$ . (a) The angular distribution of the electron density of the initial coherent state in momentum space. Shown is the momentum density of the second electron with respect to the direction of the fixed first electron. (b) The distribution of the calculated ionization signal of the second electron with respect to the direction of the fixed first electron. (c) The two-dimensional two-electron momentum space density distributions of the initial coherent state. (d) Double ionization signals showing the relative momentum distributions between the two ionized electrons (see text).

A good place to study the time-domain electron dynamics is to look for situations where the breakdown of the shell model is most severe, namely the multiply excited states of an atom. Theoretical studies in the past decades have revealed that the shell model fails completely to describe these states [9–15], and the motion of electrons in these states is better described by drawing analogy with the rotation and vibration of a floppy polyatomic molecule.

To describe the collective motion of two electrons in doubly excited states [11], it is convenient to look at the atom as a linear  $XY_2$  triatomic molecule, with X playing the role of the nucleus and Y an electron. Instead of the independent electron coordinates  $\mathbf{r}_1$  and  $\mathbf{r}_2$ , the wavefunctions are to be expressed in terms of  $R, \Omega_v = (\alpha, \theta_{12})$  for the internal stretching and bending vibrational motions, and three Euler angles  $\Omega_r = (\alpha', \beta', \gamma')$  for the overall rotational motions, respectively. Here the hyperradius  $R$  and the hyperangle  $\alpha$  are defined by  $r_1 = R \cos \alpha$  and  $r_2 = R \sin \alpha$ . Thus  $R$  stands for the size of the atom,  $\alpha$  measures the relative distance of the two electrons from the nucleus, and  $\theta_{12}$  is the angle which the two electrons make with the nucleus at the vertex. Note that each wavefunction depends on six variables excluding spins.

We now consider if one can probe the ‘instantaneous’ position or momentum correlation between the two excited electrons similar to the ‘Coulomb explosion’ in molecular ions. One possible direct method is to measure double ionization of helium by an attosecond light pulse.

We calculated the probability of double ionization by an attosecond light pulse with mean energy of 27.2 eV and pulse duration of 83 attosecond. We use a weak light pulse so that double ionization probability is calculated by the first-order perturbation theory. The two free electrons in the final states are approximated by properly symmetrized products of plane waves. Under this approximation, one can formally show that in the limit of a very

narrow pulse, the ionization probability is proportional to the two-electron charge density in the momentum space of the initial coherent state.

We have carried out a numerical calculation for the simplest coherent state made of  $2s^2 1S^e$  and  $2p^2 1S^e$ . The double ionization probability  $P(\mathbf{p}_1, \mathbf{p}_2, t)$  is a function of the six-dimensional momenta of the two electrons. This particular example of a coherent state represents a bending vibrational wave packet. In figure 4(a) we plot the ionization rate  $S(\mathbf{p}_1, \mathbf{p}_2, t) \propto P(\mathbf{p}_1, \mathbf{p}_2, t) / [\hat{\epsilon} \cdot (\mathbf{p}_1 + \mathbf{p}_2)]^2$  as a function of  $\theta_{p2}$ , with fixed ejected electron energies of two electrons  $e_1 = e_2 = 2.2$  eV and  $\theta_{p1} = 0$ , over half a period at  $t = 0, T/8, T/4, 3T/8$  and  $T/2$  attosecond (the total double ionization probability is expected to oscillate with a period of  $T = 970$  attosecond for this coherent state). Here, the angles are measured relative to the laser polarization  $\hat{\epsilon}$ . In the upper frame, the density plots constructed from the momentum space wavefunction are shown. It is clear that the angular dependence of the ionization signal resembles the angular dependence of the momentum space electron density; see figure 4(b).

In figures 4(c) and (d) we compare the ionization measurement with the momentum space densities as functions of  $\alpha_p = \arctan(p_2/p_1)$  and  $\theta_{p12} = \arccos(\hat{\mathbf{p}}_1 \cdot \hat{\mathbf{p}}_2)$ . Indeed, the ionization signal clearly reproduces the bending vibrational density of the two electrons in the momentum space. Representing the final-state wavefunctions by plane waves as in the present example is undoubtedly an over-simplification. Improved calculations might show slight distortions to the double ionization signals, a task left for future exploration.

#### 4. Summary and discussion

In this paper we show that attosecond light pulses provide a natural tool for probing atomic and electronic motions when the time scale of the physical processes is of the order of subfemtoseconds or attoseconds. Such short light pulses can also be used as a form of ‘white’ light—ideally for probing an extended wave packet in great detail. We have shown that the latter property can be used to map out the time-dependent behaviour of a vibrational wave packet of  $D_2^+$  ion after it was created by a pump pulse. From the kinetic energy release following the ionization of the  $D_2^+$  ion by an attosecond pulse versus the time delay, the full details of the vibrational wave packet can be mapped. Such measurement would provide the opportunity to extract the complete information of the initial wave packet—a task which is much more difficult to do using the time-domain measurements [16]. We have also shown that it is possible to use attosecond light pulses to probe the rotational and vibrational motions of doubly excited states of an atom. Such experiments would reveal the correlated motion of the two excited electrons in real time—a feature that is not achievable in energy-domain measurements. Such measurements in the future would allow the study of the correlated motion of a many-body systems at attosecond scale—revealing the real nature of the many-body interactions.

#### Acknowledgments

This work was supported in part by Chemical Sciences, Geosciences and Biosciences Division, Office of Basic Energy Sciences, Office of Science, US Department of Energy.

#### References

- [1] Gordon R J and Rice S A 1997 *Annu. Rev. Phys. Chem.* **48** 601
- [2] Trump C, Rottke H and Sandner W 1999 *Phys. Rev. A* **59** 2858
- [3] Posthumus J H *et al* 1999 *J. Phys. B: At. Mol. Opt. Phys.* **32** L93

- 
- [4] Pavicic D, Kiess A, Hansch T W and Figger H 2005 *Phys. Rev. Lett.* **94** 163002
  - [5] Alnaser A S *et al* 2005 *Phys. Rev. A* **72** 030702(R)
  - [6] Khare S P, Saksena V and Ojha S P 1992 *J. Phys. B: At. Mol. Opt. Phys.* **25** 2001
  - [7] Chu X and Chu S I 2001 *Phys. Rev. A* **63** 013414
  - [8] Urbain X *et al* 2004 *Phys. Rev. Lett.* **92** 163004
  - [9] Herrick D R and Sinanoğlu O 1975 *Phys. Rev.* **11** 97  
Kellman M E and Herrick D R 1980 *Phys. Rev. A* **22** 1536
  - [10] Ezra G S and Berry R S 1983 *Phys. Rev. A* **28** 1974
  - [11] Lin C D 1986 *Adv. At. Mol. Phys.* **22** 27
  - [12] Watanabe S and Lin C D 1986 *Phys. Rev. A* **34** 823
  - [13] Morishita T and Lin C D 2003 *Phys. Rev. A* **67** 022511
  - [14] Madsen L B 2003 *J. Phys. B: At. Mol. Opt. Phys.* **36** R223
  - [15] Morishita T and Lin C D 2005 *Phys. Rev. A* **71** 012504
  - [16] Andersen N, Gallagher J W and Hertel I V 1988 *Phys. Rep.* **165** 1